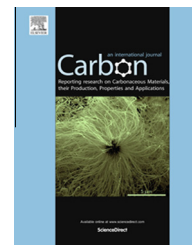


Available at www.sciencedirect.com

ScienceDirect

journal homepage: www.elsevier.com/locate/carbon

Above 170° water contact angle and oleophobicity of fluorinated graphene oxide based transparent polymeric films

T. Bharathidasan, Tharangattu N. Narayanan^{*}, S. Sathyanaryanan, S.S. Sreejakumari^{*}

CSIR-Central Electrochemical Research Institute, Karaikudi 630 006, India

ARTICLE INFO

Article history:

Received 25 September 2014

Accepted 1 December 2014

Available online 5 December 2014

ABSTRACT

Understanding and tuning the wettability of the surfaces are highly intriguing for various applications. The development of stable and transparent coatings over aluminium alloys and glass substrates for making them superhydrophobic and extended oleophobic (lower to the surface tension of 33.4 mN/m (coconut oil)) using a scalable and simple spray painting technique is demonstrated. Fluorinated graphene oxide (FGO, fluorine content of 34.4 atomic weight %), an atomically layered material, modified Polydimethylsiloxane (PDMS) polymer composite is used as the paint for the coatings. The coated films were studied for their surface and compositional features. A water contact angle (CA) of 173.7° (close to the highest ever reported water CA, 175°) is achieved with 60 wt% FGO in PDMS, and the same showing a CA of 94.9° with coconut oil, in conjunction with a low contact angle hysteresis (4°). The work of adhesion with the amount of FGO is studied and the surface energy of FGO containing paints is calculated and compared with the bare paints using Zisman plot analysis.

© 2014 Elsevier Ltd. All rights reserved.

1. Introduction

Engineering the wettability of a solid surface plays an important role in many fields such as self-cleaning surfaces, corrosion resistive coatings, and microfluidic devices [1–6]. The wettability of a solid surface by a liquid is defined in terms of the contact angle (CA), along with other factors such as tilting angle and contact angle hysteresis, and the CA is defined as the angle between the tangent plane to the surface of the solid and the tangent plane to the surface of the liquid at the point of intersection [7–9]. Surfaces with very high water (in the case where liquid is water) contact angle (>150°) are usually called superhydrophobic surfaces, while if the contact angle is below 90° the surface is called hydrophilic. The wettability of a solid

surface by a liquid is determined by the surface tension of the liquid, roughness of the solid surface and the surface energy of the solid [10–12]. Hence for a given liquid, the CA can be tuned either by creating periodically or randomly distributed micro-nanostructures and/or by engineering the surface chemistry (surface energy) of the solid. There are plenty of reports in the literature that systematically discuss the impact of surface texture on wettability [13–20].

Low-surface energy fluorine-containing polymeric coatings have been extensively studied to create superhydrophobic surfaces with water contact angle (WCA) higher than 150° due to their anti-contamination and self-cleaning properties desirable for many industrial and biological applications [21–25]. However, most of these coatings exhibit undesirably

^{*} Corresponding authors: Current address: TIFR-Centre for Interdisciplinary Sciences, Tata Institute of Fundamental Research, Hyderabad 500 075, India (T.N. Narayanan).

E-mail addresses: tn_narayanan@yahoo.com (T.N. Narayanan), sreejakumariss@gmail.com (S.S. Sreejakumari).

<http://dx.doi.org/10.1016/j.carbon.2014.12.004>

0008-6223/© 2014 Elsevier Ltd. All rights reserved.

high WCA hysteresis ($>30^\circ$) [26]. The high hysteresis may be due to: surface reorientation and chain mobility, different morphology, chemical composition heterogeneities, presence of different amounts of trapped low molecular weight polymeric species, difference in the number of surface defect sites (impurities, etc) which will influence contact angle line pinning [11,12]. Coclite et al. [27] have developed grafted crystalline poly-perfluoroacrylate structures for superhydrophobic and oleophobic functional coatings (advancing WCA = 160°) with extremely low hysteresis (5°) and oleophobicity [mineral oil (surface tension: 35 mN/m) contact angle of 108°].

The exceptional thermal and mechanical properties and excellent electrical conductivity of graphene-based sheets and films have attracted tremendous attention in recent years [28–33]. With a graphene plane decorated with hydroxyl, carbonyl, epoxy, and phenol functionalities [34], graphene oxide (GO) has shown remarkable promise as a manipulatable precursor [35]. One of the authors' and co workers have developed [36] a chemical scheme to synthesize bulk quantities of 2-dimensional (2D) nanosheets of fluorinated graphene oxide (FGO, with a fluorine content of 27 at.%), with aliphatic C–F bonds within the aromatic domain of the graphene basal plane in addition to epoxy, hydroxyl and carbonyl functional groups, which typically exist on the surface of GO. The low surface free energy of the C–F bond [37] enables one to tailor the wetting characteristics of a surface, by chemically altering the C/O and C/F ratio on the graphene oxide basal plane. But in the previous works, [36] the water contact angle was limited to 150° and oleophobicity was also limited to 92.5° (surface tension 59 mN/m). Moreover, the role of FGO was not clear from the earlier reports, since the nanomaterials can induce roughness and this can also eventually leads to the formation of air pockets. But, conventional coating techniques have no control over this roughness, in particular when composites are used as paints.

In the present work, superhydrophobic and oleophobic transparent films have been developed without the use of sophisticated patterning techniques, over a range of substrates ranging from glass to alloys using covalently functionalized FGO (having higher fluorine content than the previously reported [36] FGO) and polydimethyl siloxane (PDMS) (M_n –110,000, viscosity $\sim 50,000$ cSt) with tetraethyl ortho silicate as cross linker and dibutyltindilaureate as catalyst. In this paper, oleophobicity refers to a contact angle of greater than 90° with organic solvent (ethylene glycol) and coconut oil having surface tensions much lower than water. Though silane functionalised GO has been reported previously [38,39], here we show the covalent linkages between FGO and silane can be used for the development of stable paints/inks. The role of FGO in making self-cleaning surfaces is studied using the calculation of work of adhesion and Zisman analysis.

2. Experimental section

2.1. Materials

Polydimethylsiloxane (PDMS) silanol terminated {average molecular weight (M_n –110,000), Kinematic viscosity ($\sim 50,000$ cSt)} and Tetraethyl orthosilicate (TEOS) was

procured from Sigma Aldrich, St. Louis, United States. Fluorinated Graphite powder was procured from Sisco Research Laboratories Pvt. Ltd. from Mumbai India. Dibutyl Tin (II) laurate was procured from Alfa Aesar (A Johnson Matthey Company) from UK. Potassium permanganate, Sulphuric acid, Orthophosphoric acid, Hydrogen peroxide, Ethanol and Toluene solvents were purchased from Merck Millipore.

2.2. Synthesis

2.2.1. Preparation of fluorinated graphene oxide (FGO)

Fluorinated graphite powder was exfoliated using an 'Improved Method'. A detailed synthesis protocol has been reported [36].

2.2.2. Fabrication of PDMS–FGO composite films

The exfoliated graphene oxide was incorporated in 2.5 wt% polydimethylsiloxane (PDMS) in toluene with as received tetraethyl orthosilicate (TEOS) as cross-linker for PDMS system and dibutyl tin dilaureate as catalyst. The reaction mixtures were magnetically stirred for 30 min and spray coated over aluminium and glass substrates and maintained atomizing air pressure at 20–25 p.s.i. The thickness of the film was 8–10 μm . Fig. S3a and b in Supporting information show the distribution of various elements in FGO and PDMS–FGO film respectively.

3. Results and discussion

3.1. Wettability studies

The surface wetting property of the film depends on chemical composition, surface free energy and surface morphology and thus has an important role in achieving the desired wettability. The contact angles (CA) of the liquid droplet on the coated surface with and without incorporating varying amounts of FGO in PDMS matrix have been measured with three different liquids with varying surface tension. All measurements were made in static contact angle mode using Laplace–Young calculation method. The standard deviation of WCA was found to be $\sim \pm 0.5^\circ$. An average of 25 measurements is taken here for reporting the WCA. The polydimethylsiloxane (PDMS) film shows a water contact angle of CA – 111° (γ – 72.9 mN/m), ethylene glycol (EG) CA – 71° (γ – 47.7 mN/m) and coconut oil (C. oil) CA – 33.9° (γ – 33.4 mN/m) [all the paintings were made on an aluminium alloy which is prone for oxidation]. From this wettability study, the higher surface tension liquid water behaves as partial wetting (hydrophobic) over the PDMS film and the other two liquids are in hydrophilic array. Fig. 1A shows the variation of contact angle with concentration of FGO (wt%) in PDMS matrix (for a given FGO concentration, 5-different coated films were prepared, and in each film, CA measurements were conducted at 5 different places to show the uniformity of the coating and consistency of the CA values). Hence, the pristine PDMS surface was oleophilic, the oil CA was about 33.9° . After adding varying amount of FGO in polymer matrix, the contact angle was increased gradually, and at 60.2 wt% FGO, the PDMS–FGO film was oleophobic. The enhanced hydrophobicity and oleophobicity with fluorinated

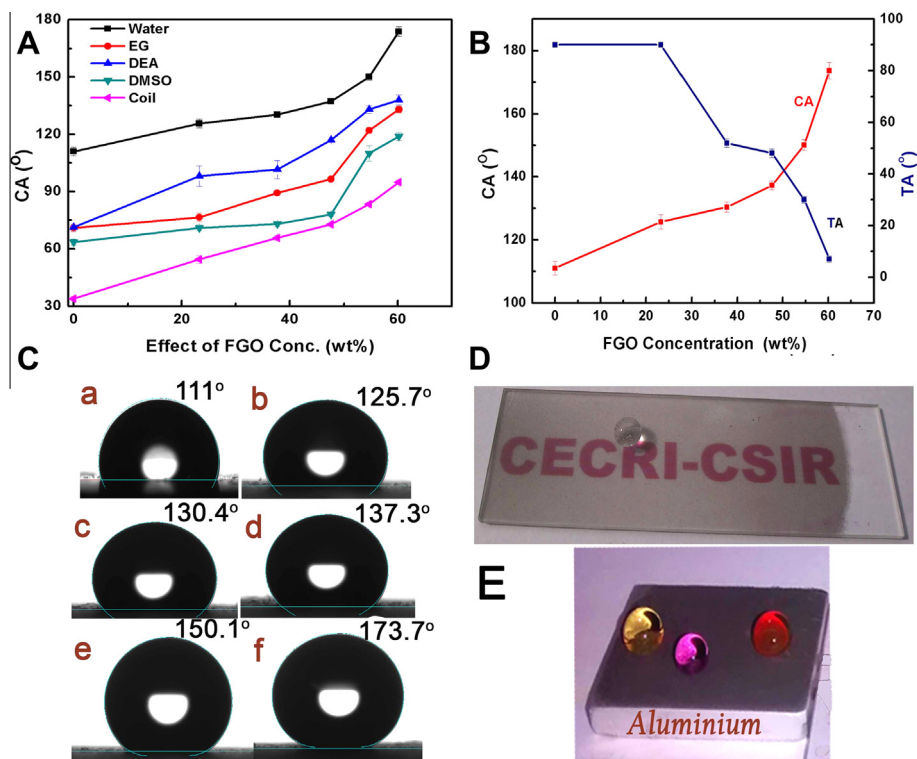


Fig. 1 – (A) Variation of contact angle of coatings with different concentration of FGO, (B) concentration of FGO versus CA and tilting angle (TA), (C) water CA Images (a – PDMS film, b – 23.3 wt%, c – 37.7 wt%, d – 47.6 wt%, e – 54.7 wt% and f – 60.2 wt% FGO in PDMS polymer matrix) [The coatings were made on an aluminium alloy] and (D) photograph of PDMS-FGO spray painted glass showing 43 % transmittance. A water droplet sitting on the coating showing a contact angle of 173.7°. (E) Coloured water (using different metal salts) droplets sitting over a coated (60 wt% FGO containing PDMS) aluminium alloy plate is shown. (A colour version of this figure can be viewed online.)

graphene oxide is attributed to the lowering of surface energy by the presence of fluorine atoms. It is seen that at 60.2 wt% FGO in PDMS matrix, the composite film exhibits superhydrophobicity (CA: 173.7°, it is close to the highest ever reported WCA (175°) [40]), with water and oleophobicity with ethylene glycol (CA: 136.2°) and coconut oil (CA: 94.9°), respectively.

Contact angle hysteresis (CAH) values of the coatings were measured by measuring the difference in dynamic contact angles (front and back of the droplet) by tilting the substrate. The CAH (average of 25 measurements in each tilting angle below 4°, where the droplet completely rolled off) is found to be 4°. The tilting of the substrate and the roll-off angle were captured in video based programming. The roll-off angle was also about 4° and the droplet was completely rolled out from the surface. The effect of FGO concentration on tilting angle (TA) is shown in the Fig. 1B. It can be seen that, above 50 wt% of FGO, the TA suddenly drops into below 20°. Fig. 1C shows the water contact angle images of pristine PDMS film and FGO Polymer composite films with different concentrations of FGO. Fig. 1D shows the photograph of a 60 wt% FGO containing PDMS-FGO film spray painted over a glass substrate. Fig. 1E shows the coloured water droplets sitting at different places of a coated (60 wt% FGO containing PDMS) aluminium alloy plate, indicating the uniform superhydrophobicity of the surface. Uniform pin-hole free coatings

can be made by this technique and the water droplets will roll off from the substrate – behaving like complete self-cleaning one (please see [Supporting information, video S2-1](#) wetting of PDMS coated glass and [video S2-2](#) non-wetting and self-cleaning of FGO modified PDMS coated glass).

PDMS film shows hydrophobicity which is explained by homogenous wetting mechanism. The homogeneity of a film has been described in terms of Wenzel equation

$$\cos\theta_r = r\cos\theta_s \quad (1)$$

This equation is used to describe the WCA for a liquid droplet on a rough solid surface [12]. Here, r is the roughness factor, and θ_r and θ_s are the WCA values on a rough surface and a smooth surface made of the same material respectively. In this regime, water is assumed to follow the roughness of the underlying surface. Here, the actual water–solid contact area is much larger than the apparent contact area. Water drops on PDMS and PDMS-FGO composite coatings up to 47.61 wt% FGO are in Wenzel state. In the case of coatings prepared with 54.7 wt% FGO, the surface exhibited non wetting and self-cleaning property with WCA of 150.2° and sliding angle (SA) < 12°. Further, in PDMS-FGO (60.2 wt%) film, the surface evinced the perfect non-wetting manner with WCA of 173.7° and sliding angle of 4°. This can be due to the transition from the Wenzel regime to Cassie regime. The roughness created on the surface with increased FGO might be

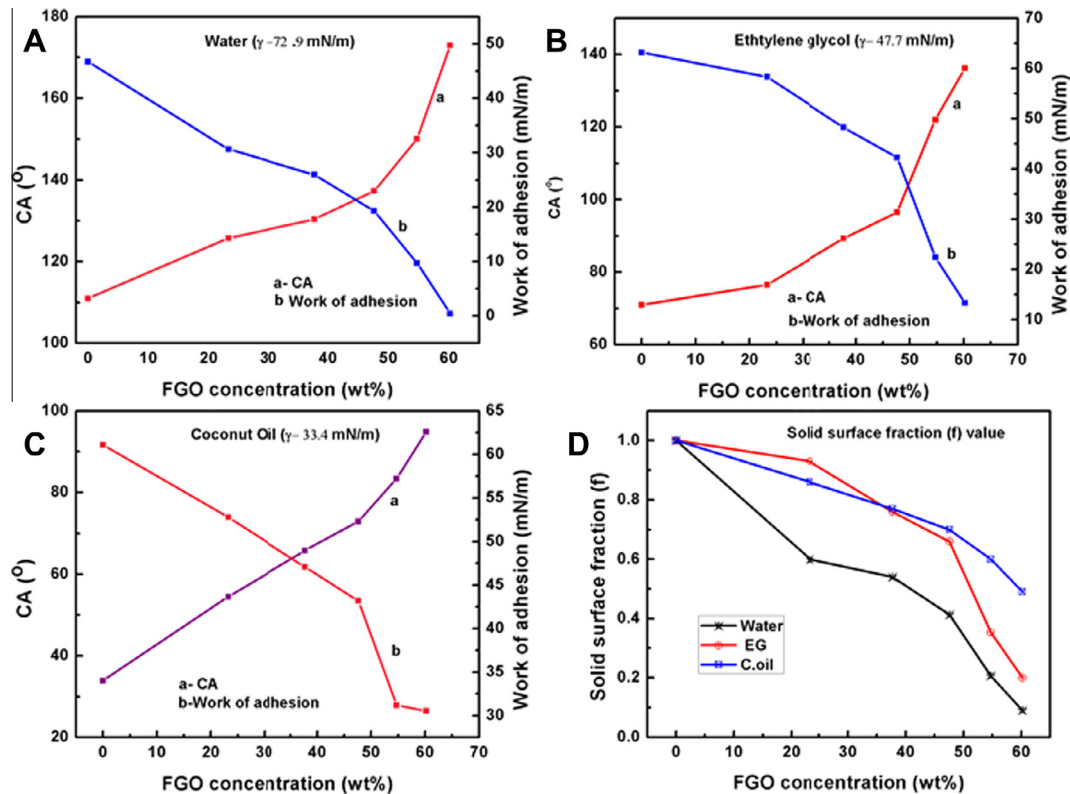


Fig. 2 – Wettability of surfaces and work of adhesion versus FGO concentration. (A) Water: $\gamma = 72.9$ mN/m, (B) ethylene glycol: $\gamma = 47.7$ mN/m, (C) coconut oil: $\gamma = 33.4$ mN/m and (D) solid surface fraction (f) value on composite films with 3 different liquids. (A colour version of this figure can be viewed online.)

sufficient to trap air inside the voids of the surface. This causes a heterogeneous surface composed of both air and solid, which reduces the adhesive force between the water and solid surface and for this case contact angle is to be described in terms of Cassie–Baxter equation.

The superhydrophobicity of PDMS–FGO composite film can be explained using Cassie’s model [11]. The CA (θ) of a drop on a heterogeneous rough surface is given by Cassie’s equation,

$$\cos\theta_r = f_1(\cos\theta_s + 1) - 1 \quad (2)$$

where f_1 is the surface area fraction of the solid, θ_r and θ_s are CA on rough and smooth surface respectively. As lot of air gets trapped into the valleys between the peaks and protrusions on the rough surface, water droplets on such coating only contacts the top of the protrusions resulting in a large water–air interface termed as composite surface which prevents water droplets from penetrating into the valleys and troughs, leading to superhydrophobicity [41]. Miwa et al. [41] have derived an equation describing the relation between WCA and SA on a rough surface and it has been shown that a very low SA is attained from a superhydrophobic surface that obeys Cassie’s model. The solid surface fraction (f) values calculated by using Cassie’s equation are found to be 1.00, 0.65, 0.55, 0.41, 0.207, and 0.0094 for 0, 23.3, 37.7, 47.6, 54.7 and 60.2 wt% respectively, as shown in the Fig. 2D. Such low solid fraction values connote for higher FGO concentrations, water droplets are exposed to an extremely large portion of air that offers a high resistance against wettability and hence

favour the movement of water droplets resulting in extremely low WSA. This can also be studied by considering the work of adhesion (W) on the surfaces. Work of adhesion basically estimates the ease with which the water drops move on the surface. The work of adhesion and solid fraction (f) values are linearly related. The work of adhesion for a smooth coating is given by the Young–Dupre’s equation [42].

$$\cos\theta = \frac{\gamma_{SA} - \gamma_{SL}}{\gamma_{LA}} = \frac{W}{\gamma_{LA}} - 1 \quad (3)$$

In Fig. 2A, the work of adhesion and contact angles for water ($\gamma=72.9$ mN/m) versus FGO concentration is plotted. The work of adhesion values are found to be 47, 30.6, 25.9, 19.3, 9.7, and 0.44 mN/m for 0, 23.3, 37.7, 47.6, 54.7 and 60.2 wt% FGO respectively. Fig. 2B and C show the WCA vs. work of adhesion of ethylene glycol and coconut oil respectively.

3.2. Surface energy calculation

Another reason for the increasing contact angle with FGO amount can be due to the lowering of surface energy due to the fluorinated materials. The contact angles of the composite films depict that surface energy of the solid films decreases which can be calculated by Zisman method [43]. The surface tension of five liquids viz., water, Diethanol Amine (DEA), Ethylene Glycol, Dimethylsulphoxide and Coconut oil with surface tension of 72.9, 48.3, 47.7, 44, and 33.4 mN/m respectively is then plotted against the cosine value of the

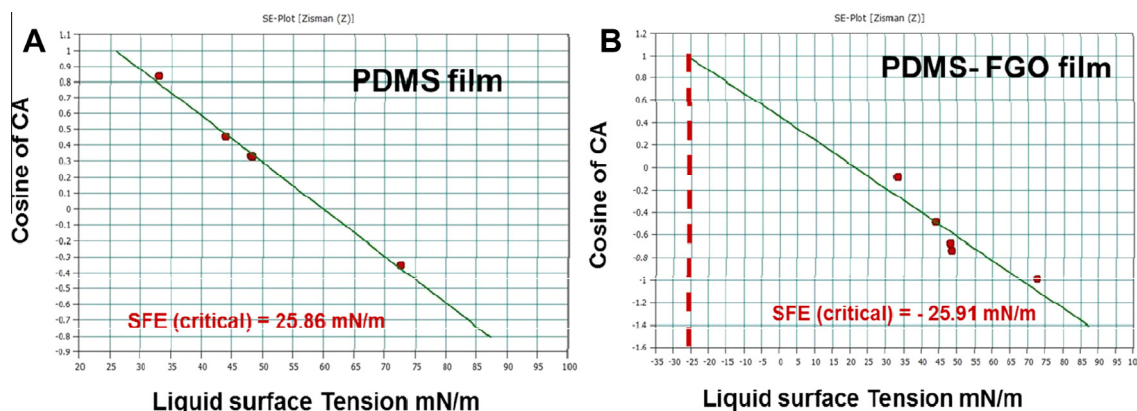


Fig. 3 – Zisman plot (A) PDMS film and (B) PDMS-FGO (60.2 wt%) film. (A colour version of this figure can be viewed online.)

corresponding contact angle which is shown in Fig. 3. The solid line in Fig. 3 represents a best fit for the measured points and is extrapolated to intersect with the value of $\text{Cos } \Theta_Y = 1$. At the point of the intersection a line (dashed line) is drawn perpendicular to the x axis and a value of critical surface tension (γ_c) is approximated to surface energy of solids [43]. The surface free energy of PDMS film calculated in the present work is 25.86 mN/m which is close to the literature value (23 mN/m) [44]. It has been observed that the surface energy gradually changes after adding FGO to polymer matrix and reduced to 18.17, 11.86, 5.78 and -15.09 with FGO concentrations of 23.3, 37.7, 47.6, and 54.7 wt% respectively (please see Supporting information for details). Further, it is seen from the Fig. 3 that surface energy has been drastically reduced (-25.91 mN/m) by adding 60.2 wt% of FGO in PDMS matrix and which is responsible for the high contact angle (173.7°).

3.3. Surface morphology

Fig. 4 shows the FESEM images of polymer films with and without FGO addition using a spray-painting technique over aluminium alloy surfaces. It is seen that the PDMS film is smooth (Fig. 4A) whereas PDMS-FGO polymeric composite film in Fig. 4B clearly shows a structure modified with layered FGO flakes. This layered structure created a number of peaks and cavities thereby roughening the surface. Such structured surfaces easily trap large amount of air within them and make the liquid droplets to rest on a layer of air.

To further probe the enhancement in the surface roughness of PDMS-FGO films, they are analysed using Atomic Force Microscopy (AFM) and the results are shown in the Supporting information Fig. S1. The pristine PDMS film is smooth with average roughness (R_a) value of 3.5 nm

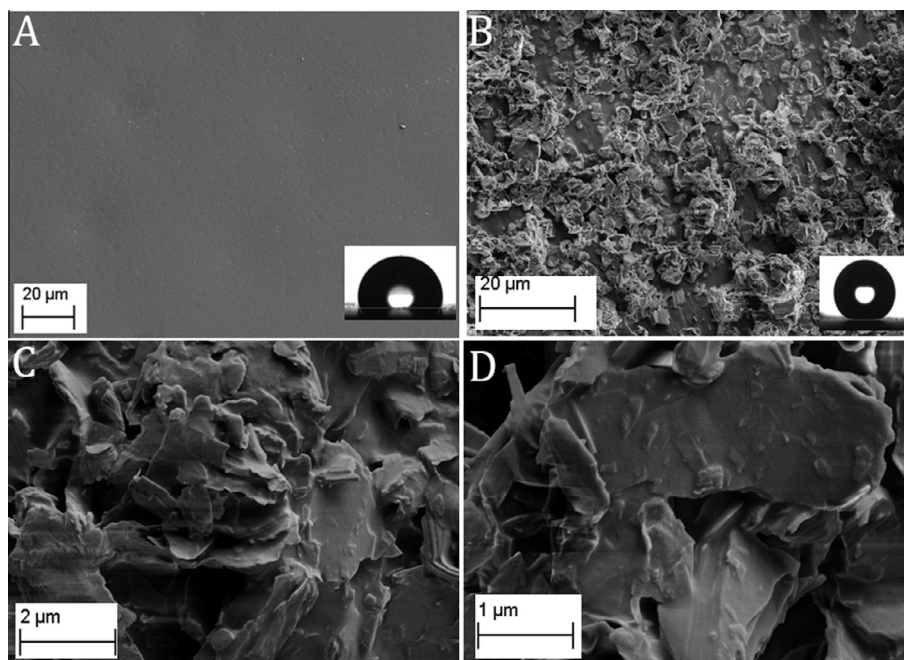


Fig. 4 – FESEM images of spray-painted aluminium alloy polymer films (A) PDMS and (B–D) PDMS-FGO film in different magnifications.

whereas the PDMS-FGO composite film shows a R_a of 245 nm.

TEM photographs (Fig. S2) of developed FGO containing 34.4 at.% F (calculated using EDX Analysis, Fig. S3) is shown in Supporting information Fig. S2. It is seen that the nano-sheets are transparent and highly stable under the electron beam. The Selected Area Electron Diffraction (SAED) pattern for FGO is shown in the Fig. S2a, indicating the hexagonal nature of FGO. 2-dimensional nature of FGO atomic layers is shown in TEM images, Fig. S2(b–d).

3.4. FT-IR studies

The chemical moieties were confirmed by FT-IR spectroscopy. The IR spectra of Graphite Monofluoride, FGO, PDMS-FGO and PDMS are shown in Fig. S4. In the Fig. S4a, the peaks at 950 and 1198 cm^{-1} correspond to C–C stretching and C–F groups respectively. In Fig. S4, the peak at 3702 cm^{-1} corresponds to free hydroxyl group in the exfoliated fluorinated graphene oxide. The peaks at 1354 and 1739 cm^{-1} correspond to C–O and C=O groups respectively. The peaks at 931, 1350 and 2965 cm^{-1} correspond to C–C stretching, C–F and C=C respectively. The peaks at 764 and 1016 cm^{-1} in Fig. S4c correspond to Si–O and Si–O–Si groups respectively and the peak at 2961 cm^{-1} corresponds to C=C bond in fluorinated graphene oxide. In Fig. S4d, the peaks at 807, 1249 and 3704 cm^{-1} correspond to Si–O, Si–CH₃ and OH groups respectively. Compared to the spectra in Fig. S4b and d, the new peak corresponding to Si–O–Si group observed in Fig. S4c indicates the covalent linkage of FGO and PDMS through the formation of Si–O bond.

These stable (paints) suspensions can be not only used as anti-corrosion coatings or self-cleaning surfaces, they can also be used for patterning, and hence to make regular hydrophilic/hydrophobic regions for applications such as water harvesting [45].

4. Conclusions

PDMS and FGO based stable ink is developed and a simple spray painting technique is used to make pin-hole free uniform coatings over a range of substrates, ranging from oxidation prone aluminium alloys to transparent glass substrates. The substrates (with 60.2 wt% FGO) showing a WCA of 173.7°, close to the highest ever reported value, with a low hysteresis of 4°. Moreover, these substrates also showed an oleophobic nature (until a surface tension of 33.4 mN/m). The role of FGO in making superhydrophobic and oleophobic surfaces is studied by varying the concentrations and the work of adhesion and surface energy of the coated substrates were compared. It is found that FGO atomic layers are not only making the surfaces rough to make enough air pockets for making Cassie–Baxter regions, but also substantially lowering the surface energy of the substrates. This study paves new dimensions for making low surface energy surfaces using stable inks containing atomically layered materials and this in turn will help to make transparent self-cleaning surfaces without the aid of sophisticated patterning techniques.

Acknowledgement

Authors thank CSIR – INDIA for the funding support in the form of CSIR network project INTELCOAT (GSC0114B).

Appendix A. Supplementary data

Supplementary data associated with this article can be found, in the online version, at <http://dx.doi.org/10.1016/j.carbon.2014.12.004>.

REFERENCES

- [1] Adamson AW. *Physical chemistry of surfaces*. New York: Wiley; 1990.
- [2] Shibuichi S, Onda T, Satoh N, Tsujii K. Super water-repellent surfaces resulting from fractal structure. *J Phys Chem* 1996;100:19512–7.
- [3] Parkin IP, Palgrave RG. Self-cleaning coatings. *J Mater Chem* 2005;15:1689–95.
- [4] Sun TL, Feng L, Gao XF, Jiang L. Bioinspired surfaces with special wettability. *Acc Chem Res* 2005;38:644–52.
- [5] De Coninck J, de Ruijter MJ, Voue M. Dynamics of wetting. *Curr Opin Colloid Interface Sci* 2001;6:49–53.
- [6] Onda T, Shibuichi S, Satoh N, Tsujii K. Super-water-repellent fractal surfaces. *Langmuir* 1996;12:2125–7.
- [7] Erbil HY. *Surface chemistry of solid and liquid interfaces*. Oxford: Wiley-Blackwell; 2006.
- [8] Ibach H. *Physics of surfaces and interfaces*. Berlin Heidelberg: Springer-Verlag; 2006.
- [9] Adamson AW, Gast AP. *Physical chemistry of surfaces*. New York: John Wiley & Sons; 1997.
- [10] Whyman G, Bormashenko E, Stein T. The rigorous derivation of Young, Cassie–Baxter and Wenzel equations and the analysis of the contact angle hysteresis phenomenon. *Chem Phys Lett* 2008;450:355–9.
- [11] Cassie ABD, Baxter S. Wettability of porous surfaces. *Trans Faraday Soc* 1944;40:546–51.
- [12] Wenzel RN. Resistance of solid surfaces to wetting by water. *Ind Eng Chem* 1936;28:988–94.
- [13] Grigoryev A, Tokarev I, Kornev KG, Luzinov I, Minko S. Superomniphobic magnetic microtextures with remote wetting control. *J Am Chem Soc* 2012;134:12916–9.
- [14] Choi W, Tuteja A, Chhatre S, Mabry JM, Cohen RE, McKinley GH. Fabrics with tunable oleophobicity. *Adv Mater* 2009;21:2190–5.
- [15] Chhatre SS, Choi W, Tuteja A, Park KC, Mabry JM, McKinley GH, et al. Scale dependence of omniphobic mesh surfaces. *Langmuir* 2010;26:4027–35.
- [16] Darmanin T, Guittard F, Amigoni S, de Givenchy ET, Noblin X, Kofman R, et al. Superoleophobic behavior of fluorinated conductive polymer films combining electropolymerization and lithography. *Soft Matter* 2011;7:1053–7.
- [17] Fujii T, Aoki Y, Habazaki H. Fabrication of super-oil-repellent dual pillar surfaces with optimized pillar intervals. *Langmuir* 2011;27:11752–6.
- [18] Hsieh CT, Wu FL, Chen WY. Superhydrophobicity and superoleophobicity from hierarchical silica sphere stacking layers. *Mater Chem Phys* 2010;121:14–21.
- [19] Zhang JP, Seeger S. Superoleophobic coatings with ultralow sliding angles based on silicone nanofilaments. *Angew Chem Int Ed* 2011;50:6652–6.

- [20] Steele A, Bayer I, Loth E. Inherently superoleophobic nanocomposite coatings by spray atomization. *Nano Lett* 2009;9:501–5.
- [21] Coulson SR, Woodward IS, Badyal JPS, Brewer SA, Willis C. Ultralow surface energy plasma polymer films. *Chem Mater* 2000;12:2031–8.
- [22] Milella A, DiMundo R, Palumbo F, Favia P, Fracassi F, d'Agostino R. Plasma nanostructuring of polymers: different routes to superhydrophobicity. *Plasma Process Polym* 2009;6:460–6.
- [23] Poly J, Ibarboure E, Rodriguez-Hernandez J, Taton D, Papon E. Reinforcing the hydrophobicity of polymeric surfaces from fluorinated star polymers and nanogels. *Macromolecules* 2010;43:1299–308.
- [24] Schmidt DL, Coburn CE, Dekoven BM, Potter GE, Meyers GF, Fischer DA. Water-based non-stick hydrophobic coatings. *Nature* 1994;368:39–41.
- [25] Ameduri B, Buotevin B. Well-architected fluoropolymers: synthesis, properties and applications. Oxford: Elsevier; 2004.
- [26] Mao Y, Gleason K. Vapor-deposited fluorinated glycidyl copolymer thin films with low surface energy and improved mechanical properties. *Macromolecules* 2006;39:3895–900.
- [27] Coclite AM, Shi Y, Gleason KK. Grafted crystalline polyperfluoroacrylate structures for superhydrophobic and oleophobic functional coatings. *Adv Mater* 2012;24:4534–9.
- [28] Singh V, Joung D, Zhai L, Das S, Khondaker SI, Seal S. Graphene based materials: past, present and future. *Prog Mater Sci* 2011;56:1178–271.
- [29] Kinam K, Jae YC, Taek K, Seong HC, Hyun JC. A role for graphene in silicon-based semiconductor devices. *Nature* 2011;479:338–44.
- [30] Compton OC, Dikin DA, Putz KW, Brinson LC, Nguyen ST. Electrically conductive “alkylated” graphene paper via chemical reduction of amine-functionalized graphene oxide paper. *Adv Mater* 2010;22:892–6.
- [31] Xu C, Wang X. Fabrication of flexible metal-nanoparticle films using graphene oxide sheets as substrates. *Small* 2009;19:2212–7.
- [32] Nair RR, Wu HA, Jayaram PN, Grigorieva IV, Geim AK. Unimpeded permeation of water through helium-leak-tight graphene-based membranes. *Science* 2012;335:442–4.
- [33] Fang M, Wang KG, Lu HB, Yang YL, Nutt S. Covalent polymer functionalization of graphene nanosheets and mechanical properties of composites. *J Mater Chem* 2009;19:7098–105.
- [34] Gao W, Alemany LB, Ci L, Ajayan PM. New insights into the structure and reduction of graphite oxide. *Nat Chem* 2009;1:403–8.
- [35] Loh KP, Bao Q, Eda G, Chhowalla M. Graphene oxide as a chemically tunable platform for optical applications. *Nat Chem* 2010;2:1015–24.
- [36] Mathkar A, Narayanan TN, Alemany LB, Cox P, Nguyen P, Gao G, et al. Synthesis of fluorinated graphene oxide and its amphiphobic properties. *Part Part Syst Char* 2013;30:266–72.
- [37] Tuteja A, Choi W, Ma ML, Mabry JM, Mazzella SA, Rutledge GC, et al. Designing superoleophobic surfaces. *Science* 2007;318:1618–22.
- [38] Hou SF, Su SJ, Kasner ML. Formation of highly stable dispersions of silane-functionalized reduced graphene oxide. *Chem Phys Lett* 2010;501:68–74.
- [39] Ou JF, Wang Y, Wang JQ, Liu S, Li ZP, Yang SR. Self-assembly of octadecyltrichlorosilane on graphene oxide and the tribological performances of the resultant film. *J Phys Chem C* 2011;115:10080–6.
- [40] <http://news.medill.northwestern.edu/chicago/news.aspx?id=227710>.
- [41] Miwa M, Nakajima A, Fujishima A, Hashimoto K, Watanabe T. Effects of the surface roughness on sliding angles of water droplets on superhydrophobic surfaces. *Langmuir* 2000;16:5754–60.
- [42] Nosonovsky M, Bhushan B. Multiscale friction mechanisms and hierarchical surfaces in nano- and bio-tribology. *Mater Sci Eng R* 2007;58:162–93.
- [43] Zisman WA. In: Gould RF, editor. Contact angle, wettability and adhesion. *Advances in chemistry series*, vol. 43. Washington, DC: American Chemical Society; 1964. p. 1–51.
- [44] Owen MJ, Petar R. *Silicone surface science*. Dvornic Springer Science and Business Media; 2012. 17.
- [45] Ozden S, Ge L, Narayanan TN, Hart AH, Yang H, Sridhar S, et al. Anisotropically functionalized carbon nanotube array based hygroscopic scaffolds. *ACS Appl Mater Interfaces* 2014;6:10608–13.